



The detection of terahertz waves by semimetallic and by semiconducting materials

F. Gouider, G. Nachtwei, C. Brüne, H. Buhmann, Yu. B. Vasilyev et al.

Citation: *J. Appl. Phys.* **109**, 013106 (2011); doi: 10.1063/1.3530727

View online: <http://dx.doi.org/10.1063/1.3530727>

View Table of Contents: <http://jap.aip.org/resource/1/JAPIAU/v109/i1>

Published by the [American Institute of Physics](http://www.aip.org).

Related Articles

Positive-negative turbulence-free ghost imaging

Appl. Phys. Lett. **100**, 131114 (2012)

Ultrahigh efficient single-crystalline TiO₂ nanorod photoconductors

Appl. Phys. Lett. **100**, 123108 (2012)

Shift of responsive peak in GaN-based metal-insulator-semiconductor photodetectors

Appl. Phys. Lett. **100**, 121109 (2012)

New Products

Rev. Sci. Instrum. **83**, 039501 (2012)

Subwavelength optical absorber with an integrated photon sorter

APL: Org. Electron. Photonics **5**, 73 (2012)

Additional information on J. Appl. Phys.

Journal Homepage: <http://jap.aip.org/>

Journal Information: http://jap.aip.org/about/about_the_journal

Top downloads: http://jap.aip.org/features/most_downloaded

Information for Authors: <http://jap.aip.org/authors>

ADVERTISEMENT

FIND THE NEEDLE IN THE HIRING HAYSTACK

Post jobs and reach thousands of hard-to-find scientists with specific skills



<http://careers.physicstoday.org/post.cfm> **physicstoday JOBS**

The detection of terahertz waves by semimetallic and by semiconducting materials

F. Gouider,^{1,a)} G. Nachtwei,¹ C. Brüne,² H. Buhmann,² Yu. B. Vasilyev,³ M. Salman,^{1,4} J. Könemann,⁵ and P. D. Buckle⁶

¹*Institut für Angewandte Physik, Technische Universität Braunschweig, Mendelssohnstr. 2, D-38106 Braunschweig, Germany*

²*Physikalisches Institut, Universität Würzburg, D-97074 Würzburg, Germany*

³*A.F. Ioffe Physical Technical Institute, Polytekhnicheskaya 26, RUS-194021 St. Petersburg, Russia*

⁴*Niedersächsische Technische Hochschule, D-38106 Braunschweig, D-38678 Clausthal-Zellerfeld, D-30167 Hannover, Germany*

⁵*Physikalisch-Technische Bundesanstalt, Bundesallee 100, D-38116 Braunschweig, Germany*

⁶*Qinetiq Ltd., Malvern WR14 3PS, United Kingdom*

(Received 19 July 2010; accepted 21 November 2010; published online 10 January 2011)

We present a survey of photoresponse (PR) measurements of various devices containing quantum wells (QWs) of HgTe of various widths d_{QW} and of InSb. By varying d_{QW} for HgTe, the material properties of the QW material change from semiconducting to semimetallic as d_{QW} is increased above a value of about 6 nm. We have studied the PR of devices made from $\text{Cd}_x\text{Hg}_{1-x}\text{Te}/\text{HgTe}/\text{Cd}_x\text{Hg}_{1-x}\text{Te}$ wafers with values of the QW width in the range of $6 \text{ nm} \leq d_{\text{QW}} \leq 21 \text{ nm}$. Only for samples with semimetallic HgTe QWs, a measurable PR could be detected. However, our investigations of samples made from $\text{Al}_x\text{In}_{1-x}\text{Sb}/\text{InSb}/\text{Al}_x\text{In}_{1-x}\text{Sb}$ wafers gave evidence that a measurable PR also can appear from devices with a semiconducting QW. Both cyclotron-resonant (CR) and nonresonant (bolometric, BO) interaction mechanisms can contribute to the PR signal. Whereas the CR contribution is dominant in $\text{Al}_x\text{In}_{1-x}\text{Sb}/\text{InSb}/\text{Al}_x\text{In}_{1-x}\text{Sb}$ samples, in $\text{Cd}_x\text{Hg}_{1-x}\text{Te}/\text{HgTe}/\text{Cd}_x\text{Hg}_{1-x}\text{Te}$ samples the behavior is more complex. In a sample with $d_{\text{QW}} = 8 \text{ nm}$, the PR is clearly dominated by the BO contribution. In the PR of another sample of $d_{\text{QW}} = 12 \text{ nm}$, both contributions (BO and CR) are present. The sample of $d_{\text{QW}} = 21 \text{ nm}$ shows a PR with not clearly separable BO and CR contributions. © 2011 American Institute of Physics. [doi:10.1063/1.3530727]

I. INTRODUCTION

The spectral range of terahertz radiation is very interesting for various applications as in medicine (imaging of dry samples), for the detection and for the identification of explosives and for the communication between computers or other devices like satellites. However, the generation, the transmission and the detection of terahertz waves is rather complicated. A frequency of 2 THz corresponds to a wavelength of about $150 \mu\text{m}$. Such high frequencies are hard to be generated by elcctronical devices (like, for example, by resonant tunneling diodes¹). The optical generation of terahertz waves, in particular of monochromatic ones, is also difficult. There is a variety of terahertz lasers like gas lasers,² quantum cascade lasers,³ free-electron lasers,⁴ or Stokes emission from Sb-doped Si samples.⁵ For our studies, we use a *p*-Ge laser^{6,7} which is continuously tunable in the wavelength range of $120 \mu\text{m} \leq \lambda \leq 180 \mu\text{m}$.⁸ The generation of broadband terahertz radiation is far easier as for example by black-body radiation of the temperature of about $T \cong 20 \text{ K}$ (heat radiation or far infrared radiation). The transmission of terahertz waves is partially obstructed by the strong absorption of photons possessing an energy E_{ph} of about 10 meV by CO_2 and H_2O molecules which have some rotation modes with corresponding quantum energy differences. As both

substances are present in atmospheric air there is an upper frequency limit of about 0.5 THz and a transmission distance limit of about 5 m for the data transfer based on terahertz radiation.⁹ There are meanwhile various detectors for terahertz radiation operating on the basis of nonresonant [(bolometric (BO))] and resonant [for example, cyclotron resonant (CR)] effects. However, detectors which are simultaneously spectrally selective and fast (response times of the order of some nanoseconds) are very difficult to realize. One possibility is the use of quantum Hall (QH) detectors.⁸ These detectors work on the basis of the Landau quantization in solids and need thus to be cooled ($T \leq 10 \text{ K}$) and to be subjected to strong magnetic fields ($B \approx 5 \text{ T}$ for samples with GaAs/ $\text{Al}_x\text{Ga}_{1-x}\text{As}$ heterojunctions, see Ref. 8). To realize QH detectors operating at lower magnetic fields ($B < 2 \text{ T}$) a possible approach is the use of devices with HgTe quantum wells (QWs), embedded in $\text{Cd}_x\text{Hg}_{1-x}\text{Te}$ barriers.^{8,10} The HgTe of the QWs behave semiconducting for $d_{\text{QW}} \leq 6 \text{ nm}$ and semimetallic for $d_{\text{QW}} \geq 6 \text{ nm}$.¹¹ In our investigations at HgTe-based detectors we found measurable photoconductivity (PC) signals only for samples with semimetallic QWs ($8 \text{ nm} \leq d_{\text{QW}} \leq 14 \text{ nm}$) and for samples with inverted band structure (again semiconducting QWs for $d_{\text{QW}} > 14 \text{ nm}$). However, the possible conclusion that the PC detection of terahertz waves needs semimetallic QW properties is wrong. In our previous studies of samples with semiconducting InSb

^{a)}Electronic mail: f.gouider@tu-bs.de.

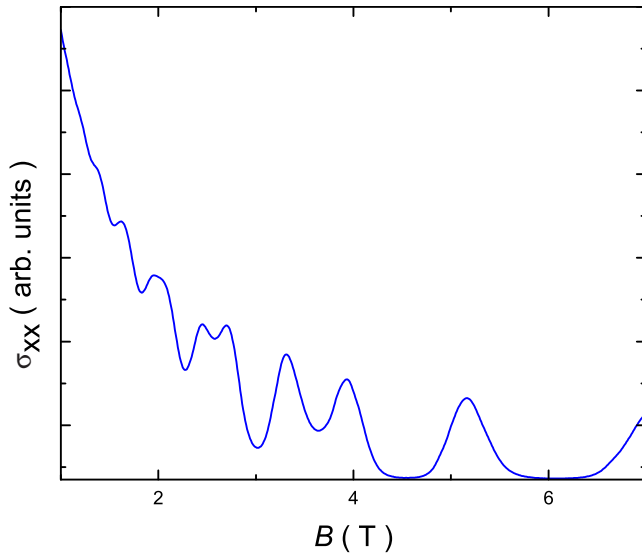


FIG. 1. (Color online) Conductivity σ_{xx} of a Corbino device patterned on a wafer with a HgTe QW with a thickness of $d_{QW}=12$ nm as a function of the magnetic field B [SdH effect].

QWs and of HgTe QWs with QWs for $d_{QW} > 14$ nm we found PC and also transmission dips at CR conditions induced by terahertz radiation.¹² Also the InSb-based samples are suitable for terahertz-QH detectors operating at $B < 2$ T. For operating terahertz detectors it is desirable to have small magnetic fields and not too low temperatures. For both material systems ($\text{Cd}_x\text{Hg}_{1-x}\text{Te}/\text{HgTe}/\text{Cd}_x\text{Hg}_{1-x}\text{Te}$ and $\text{Al}_x\text{In}_{1-x}\text{Sb}/\text{InSb}/\text{Al}_x\text{In}_{1-x}\text{Sb}$), the magnetic fields for operation can be chosen below 2 T. However, the operation of QH detectors requires a measurable energy splitting between adjacent Landau levels and thus rather low temperatures ($T \approx 4$ K, see Refs. 8, 10, and 12). Although for the operation of terahertz-QH detectors low temperatures are inevitable so far, this type of detectors possesses at least one advantage: the simultaneous occurrence of a fast response and of a spectral selectivity. The latter property is necessary for instance for the identification of substances by terahertz radiation and does not occur in bolometer detectors.

II. EXPERIMENTAL DETAILS

In this study we investigate the photoresponse (PR) in the terahertz spectral range of $\text{Cd}_x\text{Hg}_{1-x}\text{Te}/\text{HgTe}/\text{Cd}_x\text{Hg}_{1-x}\text{Te}$ (MCT) and $\text{Al}_x\text{In}_{1-x}\text{Sb}/\text{InSb}/\text{Al}_x\text{In}_{1-x}\text{Sb}$ (InSb) wafers. These wafers were grown by molecular beam epitaxy. In the following table characteristic properties of the sample are summarized:

The characteristic data n_s and μ_e are deduced from magnetotransport measurements at low temperatures ($1.5 \text{ K} \leq T \leq 4.2 \text{ K}$) and in the range of the magnetic field $0 \leq B \leq 10$ T. The PR investigations presented here are performed using our p -Ge laser emitting terahertz waves in the wavelength range $120 \mu\text{m} \leq \lambda \leq 180 \mu\text{m}$.^{8,9,12} Our laser is continuously tunable in the aforementioned wavelength range by changing the magnetic field B_{laser} (generated by a superconducting coil) at the Ge crystal in the range $2.75 \text{ T} \leq B_{laser} \leq 4.13 \text{ T}$.

TABLE I. Sample properties.

Sample No.	Sample type, d_{QW} (nm)	n_s (10^{15} m^{-2})	μ_e ($\text{m}^2/\text{V s}$)
1	MCT $d_{QW}=8$ nm	2.5	19.0
2	MCT $d_{QW}=12$ nm	4.3	1.6
3	MCT $d_{QW}=21$ nm	4.0	61.8
4	InSb $d_{QW}=30$ nm	2.8	4.2

III. EXPERIMENTAL INVESTIGATIONS

All samples were characterized before the exposure to terahertz radiation. For characterization, measurements of the Shubnikov-de Haas effect (SdH) were performed. Figure 1 shows a typical SdH curves for a HgTe Corbino sample in comparison to sample with an InSb QW.

From these measurements, the carrier density n_s and the carrier mobility μ are deduced (see, for example, Table I). Further, we measured the current-voltage (I - V) characteristics of the samples at magnetic fields corresponding to SdH minima (or integer filling factors, see Ref. 12). From the nonlinearities in the I - V curves, the operational conditions of the samples working as terahertz detectors can be determined.¹² At voltages closely below the critical value V_C of the breakdown of the QH effect (QHE), an additional optical excitation of the sample can result in completing the breakdown of the QHE.¹² The breakdown of the QHE leads to a measurable increase in the radial conductivity σ_{xx} of a Corbino device. Thus, the PC can be registered by measuring the increase in the source-drain current I_{SD} at samples pre-biased by subcritical (but high enough) source-drain voltages $V_{SD} < V_C$. Corresponding PC curves for one HgTe sample as a function of the magnetic field are shown in Fig. 2. Typically, the PC shows maximum values at the minima of $\sigma_{xx}(B)$. These maxima can be due to either nonresonant (BO) or CR contributions to the PC.¹³

In addition to the measurements of the PC, we performed transmission measurements at some of the HgTe and of the InSb wafers. For this, we placed the sample between a waveguide exit and a Ge detector.

In Fig. 3, the transmission T for terahertz waves as a function of the magnetic field is shown for a sample with a HgTe QW ($d_{QW}=8$ nm) and an InSb QW ($d_{QW}=30$ nm) for

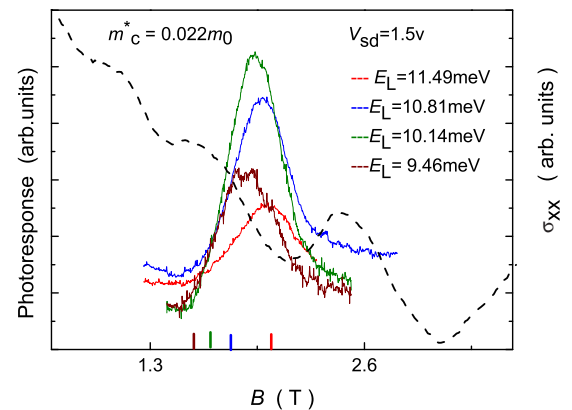


FIG. 2. (Color online) PC $\Delta\sigma_{xx}$ of the device used in Fig. 1 as a function of the magnetic field B . E_L is the energy of the photons emitted by the laser.

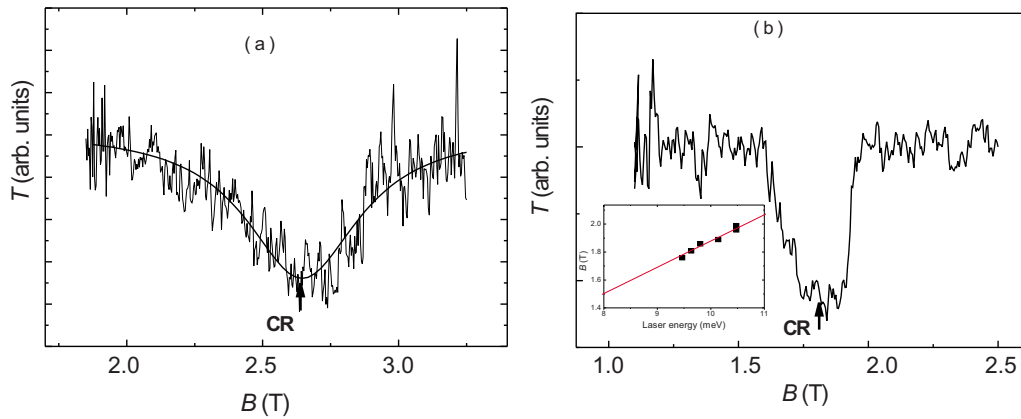


FIG. 3. (Color online) (a) Transmission T of a Corbino device patterned on a wafer with a HgTe QW with a thickness of $d_{\text{QW}}=12$ nm as a function of the magnetic field B and (b) like (a), but for a Corbino device patterned on a wafer with an InSb QW with a thickness of $d_{\text{QW}}=30$ nm. Inset: magnetic field positions of the resonance minima as a function of the photon energy for the corresponding sample.

fixed photon energies E_{ph} . In the inset of Fig. 3, the magnetic field values B_{res} of the transmission minima as a function of E_{ph} are plotted. Both for the HgTe and for the InSb samples, $E_{ph}(B_{res})$ are linear. This is typical for the CR. From the slope of $E_{ph}(B_{res})$ functions, the cyclotron mass m_c can be deduced according to:

$$E_{ph} = \hbar \frac{eB_{res}}{m_c}. \quad (1)$$

The cyclotron mass m_c is enhanced above the mass value at the energy of the bottom of the conduction band. This enhancement is due to the nonparabolic band structure $E(k)$.^{12,14} In the case of InSb samples, we can deduce the energy difference between the subband energy E_s and the Fermi energy E_F , $\Delta E = E_s - E_F$.¹² For the samples with HgTe QWs, ΔE cannot be generally determined from the corresponding m_c values. This is because of the rather complicated band structure $E(k)$ for these samples. The HgTe in QWs of thicknesses below $d_{\text{QW}}=6$ nm behave semiconducting and for $d_{\text{QW}}>6$ nm semimetallic. For $d_{\text{QW}}>14$ nm, the band structure of HgTe has again a critical point, resulting in a semiconductor with inverted band structure.¹⁵ Consequently, in our sample 3 (HgTe QW with $d_{\text{QW}}=21$ nm) the HgTe QW behaves semiconducting again. As visible in Fig. 4, for sample 3 a measurable PC occurs.

Thus, from this result and from the results obtained from the InSb samples we conclude that the PC occurs not only for semimetallic HgTe samples but also for samples with semiconducting QWs. Apart from the fact that this observation is interesting for basic physics, this knowledge is also important for the application of these devices as terahertz detectors. Our results lead to the conclusion that only samples with thin semiconducting HgTe QWs (for $d_{\text{QW}} \leq 6$ nm) are not suitable for the detection of terahertz radiation.

Whereas the results of the transmission investigations can be clearly attributed to the CR [see Eq. (1)], the electrically measured PR cannot unambiguously be attributed to either the CR (resonant excitation) or to the BO effect (nonresonant electron heating). The BO mechanism is discussed in more detail in Ref. 13. There is a possibility to check the contri-

butions of resonant and nonresonant effects to the PR. In Fig. 4 some typical results addressing this problem are shown. In color plots the value of the PR is presented as a function of the magnetic field and of the photon energy E_{ph} . These color plots are shown for four samples: three $\text{Cd}_x\text{Hg}_{1-x}\text{Te}/\text{HgTe}/\text{Cd}_x\text{Hg}_{1-x}\text{Te}$ samples with $d_{\text{QW}}=8$ nm, $d_{\text{QW}}=12$ nm, and $d_{\text{QW}}=21$ nm and for one $\text{Al}_x\text{In}_{1-x}\text{Sb}/\text{InSb}/\text{Al}_x\text{In}_{1-x}\text{Sb}$ sample with $d_{\text{QW}}=30$ nm. The linear dependencies $E_{ph}(B_{res})$ for the CR with the corresponding cyclotron masses m_c are also displayed in the corresponding plots for these four samples. For a dominating BO contribution to the PR, no dependence of the PR on the magnetic field is expected. The color plots for the $\text{Cd}_x\text{Hg}_{1-x}\text{Te}/\text{HgTe}/\text{Cd}_x\text{Hg}_{1-x}\text{Te}$ sample with $d_{\text{QW}}=8$ nm and for the $\text{Al}_x\text{In}_{1-x}\text{Sb}/\text{InSb}/\text{Al}_x\text{In}_{1-x}\text{Sb}$ sample clearly confirm this. The decrease in the PR signal for $E_{ph} < 7$ meV and for $E_{ph} > 10$ meV are due to the operational limits of our p -Ge laser. For the $\text{Cd}_x\text{Hg}_{1-x}\text{Te}/\text{HgTe}/\text{Cd}_x\text{Hg}_{1-x}\text{Te}$ sample with $d_{\text{QW}}=12$ nm (semimetallic HgTe QW) and for the $\text{Cd}_x\text{Hg}_{1-x}\text{Te}/\text{HgTe}/\text{Cd}_x\text{Hg}_{1-x}\text{Te}$ sample with $d_{\text{QW}}=21$ nm (semiconducting HgTe QW with inverted band structure) the PR behavior is more complex. In Fig. 4(b) ($d_{\text{QW}}=12$ nm) a slight dependence of the PR amplitude in the $B(E)$ plot is present. However, the dependence of the energy E_{max} of the maximum PR amplitude on the energy E does not follow the CR line. Thus, both the CR and the BO effect contribute to the PR for this sample. For the $\text{Cd}_x\text{Hg}_{1-x}\text{Te}/\text{HgTe}/\text{Cd}_x\text{Hg}_{1-x}\text{Te}$ sample with $d_{\text{QW}}=21$ nm, the behavior is even more complicated. The color plot of the PR in the $B(E)$ graph shows two maxima at about 1.2 T (9.0 meV) and at about 1.5 T (10.5 meV). These maxima are close to the CR line $E_{ph}(B_{res})$ for $m_c=0.016m_0$. Thus the PR for this sample may be strongly influenced by the CR. A clear distinction between the BO and the CR contributions to the PR is not possible in this case. This holds in particular in view of the shape of regions of higher PR amplitudes as visible in Fig. 4(c). The regions of higher PR signal values do not follow the CR line. In particular the region around 1.5 T (10.5 meV) extends toward lower energies (approximately down to 9.5 meV) at an approximately constant magnetic field. This behavior reminds of the one presented in Fig. 5(b)

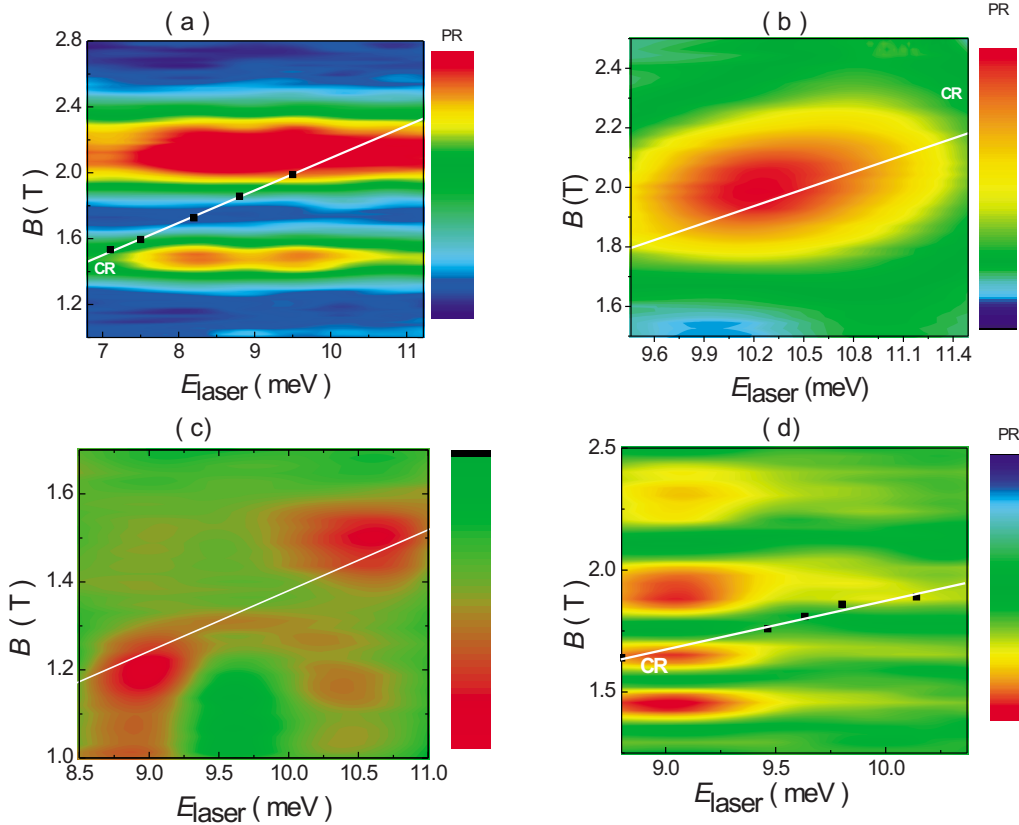


FIG. 4. (Color online) (a) PC $\Delta\sigma_{xx}$ of a Corbino device patterned on a wafer with a HgTe QW with a thickness of $d_{\text{QW}}=8$ nm as a function of the magnetic field B and of the photon energy (color plot). White line: $B_{\text{res}}(E_{\text{ph}})$ for the CR corresponding to a cyclotron mass of $m_c=0.022m_0$. (b) Like (a), but for a Corbino device with a QW thickness of $d_{\text{QW}}=12$ nm, $m_c=0.022m_0$. (c) Like (a), but for a Corbino device with a QW thickness of $d_{\text{QW}}=21$ nm, $m_c=0.016m_0$. (d) But for a Corbino device patterned on a wafer with a InSb QW with a thickness of $d_{\text{QW}}=30$ nm, $m_c=0.022m_0$.

of Ref. 8 and can be attributed to the BO effect. For the application of the devices as QH-terahertz detectors it is however not essential which effect (resonant or nonresonant) contributes dominantly to the PR. It should be noted here that a dominant BO effect does not support the operation of a QH-terahertz detector for spectroscopy. However, the BO effect can have rather short response times of the order of 10 ns for GaAs-based samples⁸ and of about 500 ns for HgTe-based samples.¹⁶

IV. SUMMARY

In this study we have compared the terahertz PR of devices with HgTe QWs of various thicknesses d_{QW} and of devices with InSb QWs of a thickness of 30 nm. For samples with HgTe QWs in the thickness range of $8 \text{ nm} \leq d_{\text{QW}} \leq 14$ nm, the HgTe behaves semimetallic. For these samples, the electrically measured PR is dominated by nonresonant heating of the carriers (bolometer effect, BO). Also samples with semiconducting QWs (InSb and HgTe of $d_{\text{QW}}=21$ nm with an inverted band structure) show a measurable PR. For these samples it cannot be clearly concluded which effect (either the nonresonant BO effect or the resonant effect (CR) dominantly contributes to the PR.

Further we measured the transmission of terahertz waves through our samples for various photon energies in the range of the operation of our laser ($6.9 \text{ meV} \leq E_{\text{ph}} \leq 10.4 \text{ meV}$). We obtained a typical CR behavior (linear increase in the

resonance magnetic field B_{res} with increasing photon energy E_{ph}) both for samples with semimetallic HgTe QWs and with semiconducting InSb QWs. From the slope of the $B_{\text{res}}(E_{\text{ph}})$ traces the cyclotron masses of electrons in the corresponding QWs were determined. These masses we found enhanced above the values of the effective masses at the band edges due to the nonparabolic dispersion relation $E(k)$ in the materials studied.

ACKNOWLEDGMENTS

Yu. B. Vasilyev acknowledges the support by the Deutsche Forschungsgemeinschaft (Project No. NA235/14). M. Salman acknowledges the support by the School for Contacts in Nanosystems of the Niedersächsische Technische Hochschule.

¹E. R. Brown, J. R. Söderström, C. D. Parker, L. J. Mahoney, K. M. Molvar, and T. C. McGill, *Appl. Phys. Lett.* **58**, 2291 (1991).

²G. A. Blake, K. B. Laughlin, R. C. Cohen, K. L. Busarow, D.-H. Gwo, C. A. Schmittenmaer, D. W. Steyert, and R. J. Saykally, *Rev. Sci. Instrum.* **62**, 1693 (1991), and references therein.

³B. S. Williams, *Nat. Photonics* **1**, 517 (2007), and references therein; S. S. Dhillon, S. Sawallich, N. Jukam, D. Oustinov, J. Madéo, S. Barbieri, P. Filloux, C. Sirtori, X. Marcadet, and J. Tignon, *Appl. Phys. Lett.* **96**, 061107 (2010).

⁴J. M. J. Madey, *J. Appl. Phys.* **42**, 1906 (1971).

⁵S. G. Pavlov, H.-W. Hübers, J. N. Hovenier, T. O. Klaassen, D. A. Carder, P. J. Phillips, B. Redlich, H. Riemann, R. K. Zhukavin, and V. N. Shastin, *Phys. Rev. Lett.* **96**, 037404 (2006).

⁶Y. L. Ivanov and Y. B. Vasilyev, *Sov. Tech. Phys. Lett.* **9**, 234 (1983).

- ⁷E. Gornik and A. A. Andronov, *Opt. Quantum Electron.* **23**, 111 (1991).
- ⁸C. Stellmach, G. Vasile, A. Hirsch, R. Bonk, Y. B. Vasilyev, G. Hein, C. R. Becker, and G. Nachtwei, *Phys. Rev. B* **76**, 035341 (2007).
- ⁹J. M. Guldbakke, Diploma thesis, Technical University of Braunschweig, 2004.
- ¹⁰S.-C. Zhang, B. A. Bernevic, and T. Hughes, A12.00013 March Meeting of the American Physical Society, Vol. 52, Denver, Colorado, USA, March 5–9, 2007.
- ¹¹M. von Truchseß, Ph.D. thesis, University of Würzburg, 1999.
- ¹²F. Gouider, Y. B. Vasilyev, M. Bugár, J. Könnemann, P. D. Buckle, and G. Nachtwei, *Phys. Rev. B* **81**, 155304 (2010).
- ¹³G. Nachtwei, F. Gouider, C. Stellmach, G. Vasile, Y. B. Vasilyev, G. Hein, and R. R. Gerhardt, *Phys. Rev. B* **78**, 174305 (2008).
- ¹⁴E. O. Kane, *J. Phys. Chem. Solids* **1**, 249 (1957).
- ¹⁵F. Gouider, Yu. B. Vasilyev, M. Bugár, J. Könnemann, C. Brüne, H. Buhmann, and G. Nachtwei, Proceedings of 16th International Conference on Electron Dynamics in Semiconductors, Optoelectronics, and Nanostructures, EDISON 16, Montpellier, France, August 24–28, 2009.
- ¹⁶R. Bonk, Diploma thesis, Technical University of Braunschweig, 2006.